Ocean Engineering 147 (2018) 215–226

Contents lists available at ScienceDirect

Ocean Engineering

journal homepage: www.elsevier.com/locate/oceaneng

An empirical formula for maximum wave setup based on a coupled wave-current model

Chao Ji [a], Qinghe Zhang [a,*], Yongsheng Wu [b]

[a] State Key Laboratory of Hydraulic Engineering Simulation and Safety, Tianjin University, Tianjin, 300072, China
[b] Marine Ecosystem Section, Ocean Ecosystem Sciences Division, Fisheries and Oceans Canada, Bedford Institute of Oceanography, Dartmouth, Nova Scotia, B2Y 4A2, Canada

ARTICLE INFO

Keywords:
Random waves
Wave setup
Wave-current interaction
SWAN
FVCOM

ABSTRACT

The present paper proposes an empirical formula for maximum wave setup based on a coupled wave-current model. The wave model is the Simulating Waves Nearshore (SWAN) model; the current model is the Finite Volume Community Ocean Model (FVCOM). This study first evaluates the coupled model system against mean water level data collected from a series of laboratory and field experiments. The model calculation agrees with the measurements. Then, the study uses the model results from simulations with a range of wave conditions to develop an empirical formula for the maximum wave setup as a function of wave height, wavelength in deep water, and beach slope. The formula agrees with experimental and *in situ* measurements and shows better performance than previous formulas.

1. Introduction

Wave setup (or setdown), defined as an increase (or decrease) in the mean water level with the presence of waves, is a common dynamic process in the nearshore zone (Lentz and Raubenheimer, 1999). Wave setup dynamics is important for understanding many coastal phenomena, such as sediment transport and wave-structure interaction (Calabrese et al., 2008; Hu et al., 2009). The maximum wave setup elevation is a key criterion for coastal protection and coastal flooding prediction (Guza and Thornton, 1981; Nielsen, 1988).

Since the mid-20th century, researchers have investigated wave setup using theoretical, experimental and numerical methods. Considering the radiation stress caused by regular waves, e.g., Longuet-Higgins and Stewart (1964, hereinafter LHS) derived an analytical solution for the horizontal gradient of the mean sea level along the offshore direction:

$$\frac{d\eta}{dx} = -K\tan\beta\,, \quad K = \frac{1}{1+8/3\gamma_b^2} \tag{1}$$

where η is the mean water level, x is the offshore coordinate, β represents the angle of the beach slope, and γ_b is the ratio of wave height-to-water depth at breaking and is assumed to be constant. With the assumption that β = constant and the solution of Eq. (1), Battjes (1974) showed that the maximum wave setup value would occur on a beach characterized by the following expression:

$$\eta_{\max} = \frac{5}{16}\gamma_b H_b \tag{2}$$

where H_b is the wave height at the breaking line.

Based on laboratory experiments, Bowen et al. (1968) and Van Dorn (1976) studied the maximum setup properties of monochromatic waves with wave flumes, and they found that the LHS theory agreed with their experiments. Battjes (1972, 1974) investigated the wave setup of random waves using laboratory experiments. They concluded that the maximum setup was somewhat lower than that predicted by the LHS theory, most likely because the theory ignored variation in γ_b. Since then, several studies have produced field observations (e.g., Guza and Thornton, 1981; Nielsen, 1988; Raubenheimer et al., 2001; Stockdon et al., 2006). Based on *in situ* data from natural, gently sloping beaches in southern California, Guza and Thornton (1981) proposed the following expression of the maximum mean water level:

$$\eta_{\max} = 0.17H_{0,s} \tag{3}$$

* Corresponding author.
E-mail address: qhzhang@tju.edu.cn (Q. Zhang).

https://doi.org/10.1016/j.oceaneng.2017.10.021
Received 24 June 2016; Received in revised form 1 September 2017; Accepted 15 October 2017
Available online 5 November 2017

where $H_{0,s}$ is the significant wave height (the average height of the highest one-third of waves or four times the standard deviation of the time series of sea-surface elevation) in deep water. Later studies extended Eq. (3) to a more general relationship including the Iribarren number (Nielsen, 1988; Stockdon et al., 2006):

$$\eta_{\max} \propto H_{0,s}\xi_0 \tag{4}$$

in which $\xi_0 = \tan\beta/\sqrt{H_{0,s}/L_0}$ is the Iribarren number and L_0 is the wavelength in deep water obtained using the peak wave period. Holman and Sallenger (1985) reported an empirical regression equation for the maximum setup value based on the data collected by field experiments under middle tide conditions:

$$\frac{\eta_{\max}}{H_{0,s}} = 0.46\xi_0 \tag{5}$$

Hanslow and Nielsen (1992) produced the following empirical equation based on field measurements along the New South Wales coast:

$$\eta_{\max} = 0.048(H_{0,rms}L_{0,s})^{0.5} \tag{6}$$

where $H_{0,rms}$ is the root mean square wave height in deep water and $L_{0,s}$ is the wavelength in deep water computed using the significant period (the average period of the highest one-third of waves). The wave heights are assumed to obey the Rayleigh distribution in deep water, indicating that $H_{0,rms} = H_{0,s}/\sqrt{2}$ (Battjes and Groenendijk, 2000). Using datasets from ten field experiments over a range of beach and wave conditions, Stockdon et al. (2006) developed an empirical formulation for the maximum wave setup using an Iribarren-like form:

$$\eta_{\max} = 0.35\tan\beta(H_{0,s}L_0)^{0.5} \tag{7}$$

Although researchers have presented expressions of the maximum wave setup for both monochromatic and random waves, most of the expressions for random waves are empirical formulas fitted to field observation data collected from limited places and times. Therefore, studies have yet to explore the broad applicability of these formulas.

Recently, researchers have increasingly used numerical models to simulate wave dynamics in idealized or realistic situations. For instance, Wolf et al. (1988) developed a coupled model to investigate the interactions between waves and tides or surges. Schäffer et al. (1993) and Madsen et al. (1997a, 1997b) simulated wave dynamics in the surf zone using a Boussinesq-type model and obtained good agreement between the model results and measurements. More recently, Mellor et al. (2008) developed a coupled wave-circulation model to consider the influences of wave-induced radiation stress on ocean circulation. Warner et al. (2008) developed a coupled wave-current-sediment model to stress the role of waves on sediment transport in estuaries and coastal waters. Kumar et al. (2012) implemented vortex force formalism in the coupled ocean-atmosphere-wave-sediment transport modeling system (COAWST). Numerical models involve solving variations in wave parameters with time and space via a set of momentum and energy conservation equations with forcing, boundary and initial conditions. In contrast to field observations, where forcing conditions are complex, researchers can use numerical models to study wave dynamics under controlled forcing conditions based on specific purposes. Accordingly, this study investigates maximum wave setup using a coupled wave-current model.

The arrangement of the present paper is as follows. Section 2 describes the model setup and verification. Section 3 presents the model results and an empirical formula for the maximum wave setup. Section 4 shows the evaluation of this formula. Section 5 provides a discussion of the limitations of this approach and comparisons between this empirical formula and several previous formulations. Finally, Section 6 presents the conclusions.

2. Model description

2.1. Model framework

The present study applies a coupled wave-current model system that includes the Simulating Waves Nearshore (SWAN) wave model and the Finite Volume Community Ocean Model (FVCOM) circulation model. Information exchange between the two models uses Model-Coupling Toolkit (MCT) software (Jacob et al., 2005; Larson et al., 2005). The present investigation uses MCT to couple SWAN and FVCOM following the method of Yang (2012) and runs the two models on the same unstructured grid. Both SWAN and FVCOM run on their set of processors in the coupled system and exchange information based on a defined time interval depending on computational power and the temporal scales of the specific wave and circulation conditions. Fig. 1 shows the information exchange between SWAN and FVCOM. The coupled model system runs on Linux platforms. FVCOM uses the wave parameters transferred from SWAN to calculate the force in the form of wave-induced radiation stress gradients and to generate the currents and wave setup. SWAN uses the currents and water levels transferred from FVCOM to include current and water level change effects on wave transformation and breaking processes. Finally, the wave setup is numerically established after reaching a steady state. The maximum wave setup is defined as the mean water level elevation at the interaction between wetting and drying on the beach face. In the model run, the minimum grid spacing is 1/7 to 1/20 of the shoreline advancement landward in the horizontal direction and is small enough to be suitably accurate for the maximum setup.

2.2. Wave model

SWAN is a third-generation wave model developed by Delft University and is a fully discrete spectral model based on the action balance equation (Booij et al., 1999). The mean rate of energy dissipation per unit horizontal area as a result of wave breaking uses the results of Battjes and Janssen (1978) based on the following expression:

$$D_{\text{tot}} = -\frac{1}{4}\alpha_{\text{BJ}}Q_b\left(\frac{\overline{\sigma}}{2\pi}\right)H_{\max}^2 \tag{8}$$

where the coefficient $\alpha_{\text{BJ}} = 1$, $\overline{\sigma}$ is the mean frequency, and Q_b is the fraction of breaking waves and is computed as follows:

$$\frac{1-Q_b}{\ln Q_b} = -8\frac{E_{\text{tot}}}{H_{\max}^2} \tag{9}$$

where E_{tot} is the total wave energy. The maximum wave height $H_{\max}$ is determined in SWAN via $H_{\max} = \gamma_b d$, in which γ_b is the breaker index and

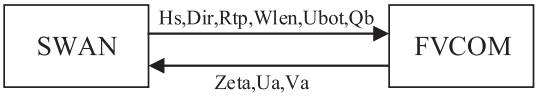

Fig. 1. Information exchange between model components. SWAN provides wave parameters, including significant wave height (Hs), wave direction (Dir), peak wave period (Rtp), wavelength (Wlen), bottom orbital velocity (Ubot) and fraction of breaking waves (Qb), to FVCOM. FVCOM provides water elevation (Zeta) and depth-averaged current fields (Ua and Va) to SWAN.

Table 1
Experimental conditions employed.

Literature	Wave type	H_{rms} (m)	D (m)	T_p (sec)	tanβ	θ
Stive (1985)	Random	1.00	4.19	5.41	1:40	0°
Ting (2001)	Random	0.22	0.46	2.00	1:35	0°
Shen (2015)	Random	0.026	0.18	1.50	1:100	30°
Scott et al. (2004)	Random	0.76	0.42	4.00	Non-uniform	0°

Table 2
Selected model control parameters.

Model component	Parameter	Value used
SWAN	Peak enhancement factor for JONSWAP spectrum	3.3
	Threshold depth	0.005 m
	Bottom friction coefficient	0.001 m^2/sec^3
FVCOM	Ratio of internal time step to external time step	10
	Threshold depth for the wet/dry treatment	0.005 m
	Coefficient used in the Smagorinsky parameterization	0.1
	Bottom roughness length scale	0.001 m

d is the water depth. Then, the spectral dependent energy dissipation is calculated as follows:

$$S_{ds,br}(\sigma,\theta) = \frac{D_{tot}}{E_{tot}} E(\sigma,\theta) \tag{10}$$

where $E(\sigma,\theta)$ is the energy density spectrum.

Following Goda (1970, 2009), the breaker index is defined as follows:

$$\gamma_b = A\left\{1 - \exp\left[-1.5\frac{\pi d_b}{L_0}\left(1 + 15\tan^{4/3}\beta\right)\right]\right\}\Big/\frac{d_b}{L_0} \tag{11}$$

where A is the breaking coefficient, and d_b is the water depth at the breaking of the wave.

The value of A is given by the expression below according to the study of Shen et al. (2015):

$$A = 0.228 \times \left(\frac{H_0}{L_0}\right)^{0.108} \tag{12}$$

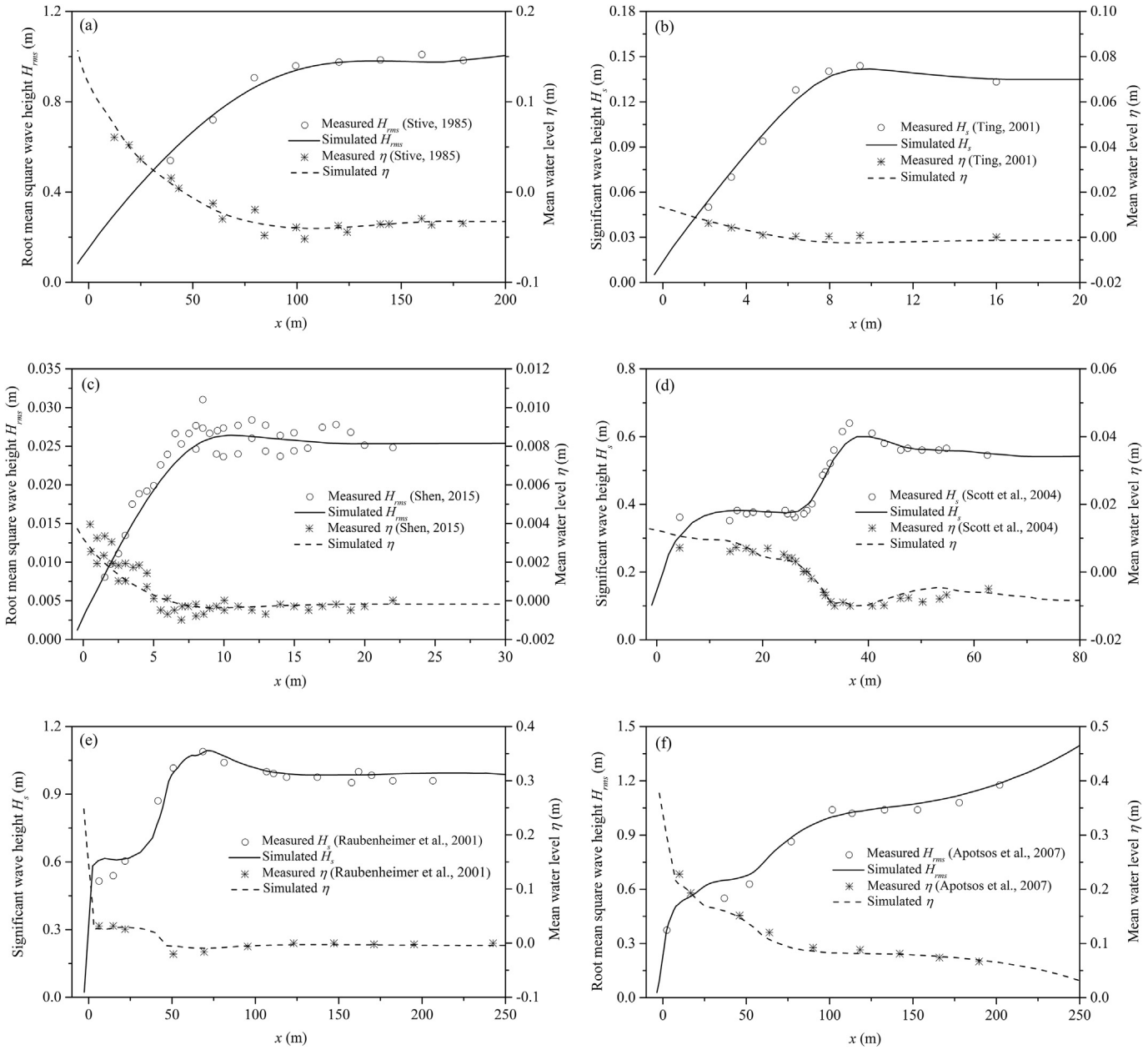

Fig. 2. Simulated wave height and mean water level compared with measured data. The x-coordinate is the distance from the intersection of the still water level and the beach slope. The use of H_{rms} or H_s in subfigures is dependent on the original data in the literature.

Table 3
Statistical measures for simulated results.

Literature		I_a	CC	MBE (10^{-2} m)	$RMSE$ (10^{-2} m)	$RRMSE$
Stive (1985)	Root mean square wave height	0.99	0.99	−0.53	2.50	0.03
	Mean water level	0.99	0.98	0.10	0.69	0.19
Ting (2001)	Significant wave height	0.99	0.99	0.02	0.42	0.04
	Mean water level	0.90	0.95	−0.09	0.18	0.62
Shen (2015)	Root mean square wave height	0.97	0.94	−0.07	0.19	0.08
	Mean water level	0.94	0.93	−0.01	0.06	0.39
Scott et al. (2004)	Significant wave height	0.99	0.98	−0.33	2.11	0.04
	Mean water level	0.98	0.97	0.07	0.17	0.24
Raubenheimer et al. (2001)	Significant wave height	0.98	0.98	1.36	3.77	0.04
	Mean water level	0.97	0.95	0.04	0.56	0.06
Apotsos et al. (2007)	Root mean square wave height	0.99	0.99	2.40	4.25	0.05
	Mean water level	0.99	0.99	−0.51	0.84	0.06

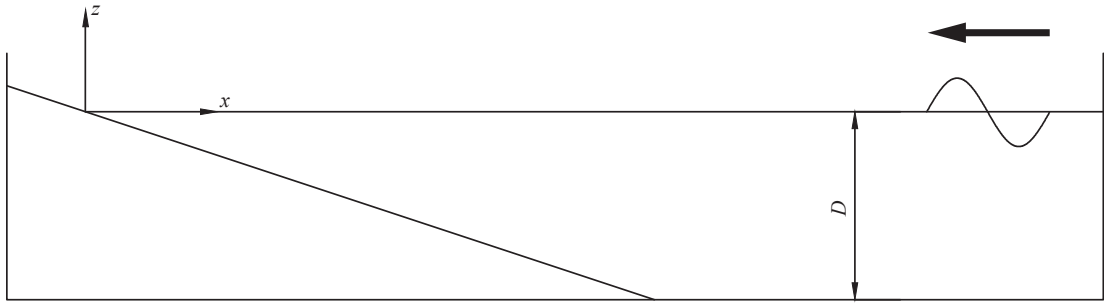

Fig. 3. The diagram of idealized test cases. The thick arrow represents the direction of wave propagation, and D represents the water depth before the slope.

This study added Eqs. (11) and (12) to the SWAN model to determine the breaker index based on the wave parameters, water depth and slope. The SWAN model with the modified Goda formula can provide good predictions of nearshore random wave breaking without manually adjusting the parameters of the breaker index (Shen et al., 2015).

2.3. Circulation model

The circulation model is FVCOM (Chen et al., 2003, 2007). The primary governing equations in the terrain-following coordinate, including the influence of waves, are as follows:

Table 4
Model input conditions for idealized test cases.

Case number	H_{rms} (m)	D (m)	T_p (sec)	tanβ	Case number	H_{rms} (m)	D (m)	T_p (sec)	tanβ
Test 1	0.2	8.0	6.0	1:10	Test 2	1.0	8.0	6.0	1:10
Test 3	2.0	8.0	5.0	1:10	Test 4	2.2	8.0	4.0	1:10
Test 5	1.8	8.0	3.0	1:10	Test 6	2.3	8.0	3.0	1:10
Test 7	0.2	8.0	6.0	1:15	Test 8	1.0	8.0	6.0	1:15
Test 9	2.0	8.0	5.0	1:15	Test 10	2.2	8.0	4.0	1:15
Test 11	1.8	8.0	3.0	1:15	Test 12	2.3	8.0	3.0	1:15
Test 13	0.2	8.0	6.0	1:25	Test 14	1.0	8.0	6.0	1:25
Test 15	2.0	8.0	5.0	1:25	Test 16	2.2	8.0	4.0	1:25
Test 17	1.8	8.0	3.0	1:25	Test 18	2.3	8.0	3.0	1:25
Test 19	0.2	8.0	6.0	1:35	Test 20	1.0	8.0	6.0	1:35
Test 21	2.0	8.0	5.0	1:35	Test 22	2.2	8.0	4.0	1:35
Test 23	1.8	8.0	3.0	1:35	Test 24	2.3	8.0	3.0	1:35
Test 25	0.2	8.0	6.0	1:50	Test 26	0.5	8.0	6.0	1:50
Test 27	1.0	8.0	6.0	1:50	Test 28	1.5	8.0	6.0	1:50
Test 29	2.0	8.0	6.0	1:50	Test 30	2.5	8.0	6.0	1:50
Test 31	1.0	8.0	2.0	1:50	Test 32	1.0	8.0	4.0	1:50
Test 33	1.0	8.0	8.0	1:50	Test 34	1.0	8.0	10.0	1:50
Test 35	1.0	8.0	12.0	1:50	Test 36	1.0	8.0	14.0	1:50
Test 37	0.6	8.0	2.0	1:50	Test 38	0.8	8.0	2.0	1:50
Test 39	1.4	8.0	4.0	1:50	Test 40	1.8	8.0	4.0	1:50
Test 41	3.0	8.0	8.0	1:50	Test 42	3.0	8.0	10.0	1:50
Test 43	3.0	8.0	12.0	1:50	Test 44	3.0	8.0	14.0	1:50
Test 45	1.0	10.0	6.0	1:50	Test 46	0.2	8.0	6.0	1:100
Test 47	1.0	8.0	6.0	1:100	Test 48	2.0	8.0	5.0	1:100
Test 49	2.2	8.0	4.0	1:100	Test 50	1.8	8.0	3.0	1:100
Test 51	2.3	8.0	3.0	1:100	Test 52	0.2	8.0	6.0	1:200
Test 53	1.0	8.0	6.0	1:200	Test 54	2.0	8.0	5.0	1:200
Test 55	2.2	8.0	4.0	1:200	Test 56	1.8	8.0	3.0	1:200
Test 57	2.3	8.0	3.0	1:200					

$$\frac{\partial \eta}{\partial t}+\frac{\partial Du}{\partial x}+\frac{\partial Dv}{\partial y}+\frac{\partial w}{\partial \sigma}=0 \tag{13}$$

$$\begin{aligned}&\frac{\partial uD}{\partial t}+\frac{\partial u^2D}{\partial x}+\frac{\partial uvD}{\partial y}+\frac{\partial uw}{\partial \sigma}-fvD\\&=-gD\frac{\partial \eta}{\partial x}-\frac{gD}{\rho_0}\left[\frac{\partial}{\partial x}\left(D\int_\sigma^0\rho d\sigma'\right)+\sigma\rho\frac{\partial D}{\partial x}\right]+\frac{1}{D}\frac{\partial}{\partial \sigma}\left(K_m\frac{\partial u}{\partial \sigma}\right)+DF_x\\&-\frac{\partial(DS_{xx})}{\partial x}-\frac{\partial(DS_{xy})}{\partial y}+\frac{\partial S_{px}}{\partial \sigma}-\frac{\partial(DR_{xx})}{\partial x}-\frac{\partial(DR_{xy})}{\partial y}\end{aligned} \tag{14}$$

$$\begin{aligned}&\frac{\partial vD}{\partial t}+\frac{\partial uvD}{\partial x}+\frac{\partial v^2D}{\partial y}+\frac{\partial vw}{\partial \sigma}+fuD\\&=-gD\frac{\partial \eta}{\partial y}-\frac{gD}{\rho_0}\left[\frac{\partial}{\partial y}\left(D\int_\sigma^0\rho d\sigma'\right)+\sigma\rho\frac{\partial D}{\partial y}\right]+\frac{1}{D}\frac{\partial}{\partial \sigma}\left(K_m\frac{\partial v}{\partial \sigma}\right)+DF_y\\&-\frac{\partial(DS_{yx})}{\partial x}-\frac{\partial(DS_{yy})}{\partial y}+\frac{\partial S_{py}}{\partial \sigma}-\frac{\partial(DR_{yx})}{\partial x}-\frac{\partial(DR_{yy})}{\partial y}\end{aligned} \tag{15}$$

in which D represents the total water depth and $D = H + \eta$, where H is the bottom depth and η is the height of the free surface; u, v and w are the x, y and σ velocity components, respectively; f is the Coriolis parameter; g is the gravitational acceleration; ρ and ρ_0 are the total and reference densities, respectively; K_m is the vertical eddy viscosity coefficient parameterized using the MY-2.5 turbulence submodel (Mellor and Yamada, 1982); F_x and F_y represent horizontal momentum diffusion terms; S_{xx}, S_{xy}, S_{yx}, and S_{yy} are horizontal radiation stress terms; S_{px} and S_{py} are vertical radiation stress terms; R_{xx}, R_{xy}, R_{yx}, and R_{yy} are surface roller terms (Svendsen, 1984); and σ is the vertical sigma coordinate and is defined as follows:

$$\sigma=\frac{z-\eta}{H+\eta}=\frac{z-\eta}{D} \tag{16}$$

The two alternative representations of the wave effects on coastal waters are radiation stress and vortex force (Bennis et al., 2011; Kumar et al., 2012). Previous studies (Kumar et al., 2012; Moghimi et al., 2013) have shown that these two representations are in general agreement regarding wave setup, which is the focus in the present paper. Here, FVCOM employed the equations of Mellor (2003). Mellor (2013, 2015) provided a corroborative and simpler derivation of the vertically dependent equations of radiation stress; certain details in Mellor (2003) were corrected (see http://shoni2.princeton.edu/ftp/glm/Corrected2003.pdf). This model included the radiation stress caused by waves using the theory of Mellor (2015):

$$S_{xx}=kE\left(\frac{k_xk_x}{k^2}F_{cs}F_{cc}-F_{ss}F_{sc}\right)+\frac{E}{2D}\frac{\partial}{\partial \sigma}\left(2F_{cc}F_{ss}-F_{ss}^2\right) \tag{17}$$

$$S_{yy}=kE\left(\frac{k_yk_y}{k^2}F_{cs}F_{cc}-F_{ss}F_{sc}\right)+\frac{E}{2D}\frac{\partial}{\partial \sigma}\left(2F_{cc}F_{ss}-F_{ss}^2\right) \tag{18}$$

$$S_{xy}=S_{yx}=kE\left(\frac{k_xk_y}{k^2}F_{cs}F_{cc}\right) \tag{19}$$

in which k is the wave number; k_x and k_y are the wave number components in the x and y directions, respectively; and E is the wave energy. The vertical distribution functions are calculated as follows:

$$F_{ss}=\frac{\sinh kD(1+\sigma)}{\sinh kD} \tag{20}$$

$$F_{cs}=\frac{\cosh kD(1+\sigma)}{\sinh kD} \tag{21}$$

$$F_{sc}=\frac{\sinh kD(1+\sigma)}{\cosh kD} \tag{22}$$

$$F_{cc}=\frac{\cosh kD(1+\sigma)}{\cosh kD} \tag{23}$$

2.4. Model verification

This section describes the verification of the coupled model system with experimental data from the literature. Table 1 lists the experiments. The present investigation also includes field measurements of the SandyDuck experiment (the field data are from Raubenheimer et al. (2001) and Apotsos et al. (2007)) to verify the model. The model simulations use default values and options for most model control parameters. Table 2 presents the selected model parameters.

Fig. 2 shows the comparison of simulated wave height and mean

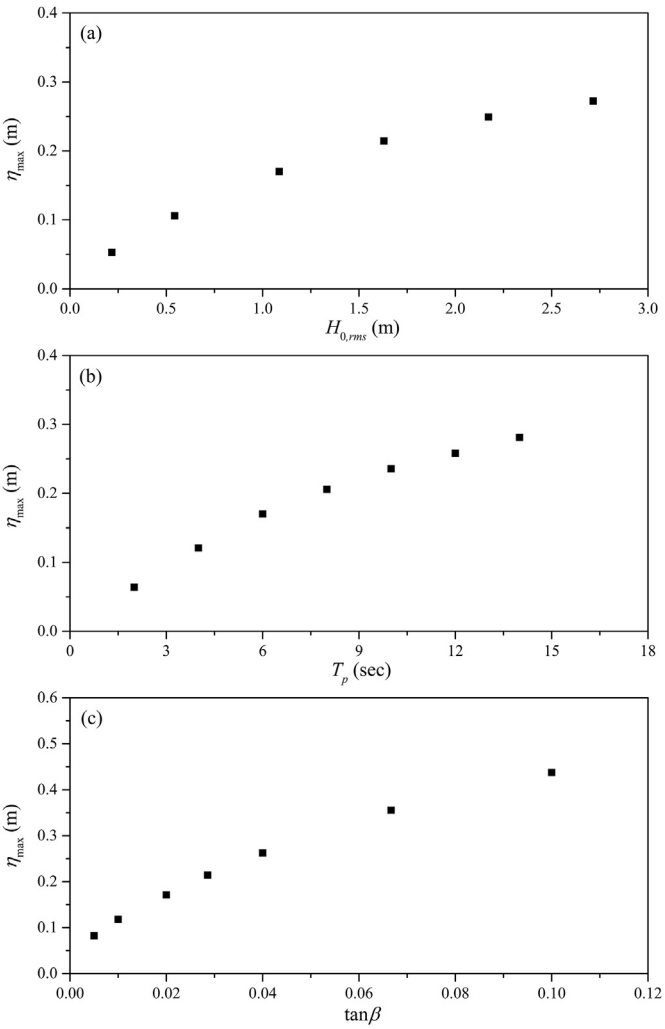

Fig. 4. Relationships between the maximum wave setup and the wave height, peak period and slope. $H_{0,rms}$ represents the root mean square wave height for random waves in deep water; it is obtained from the incident wave height through the conservation of wave energy flux using linear wave theory. η_{max} is the maximum wave setup.

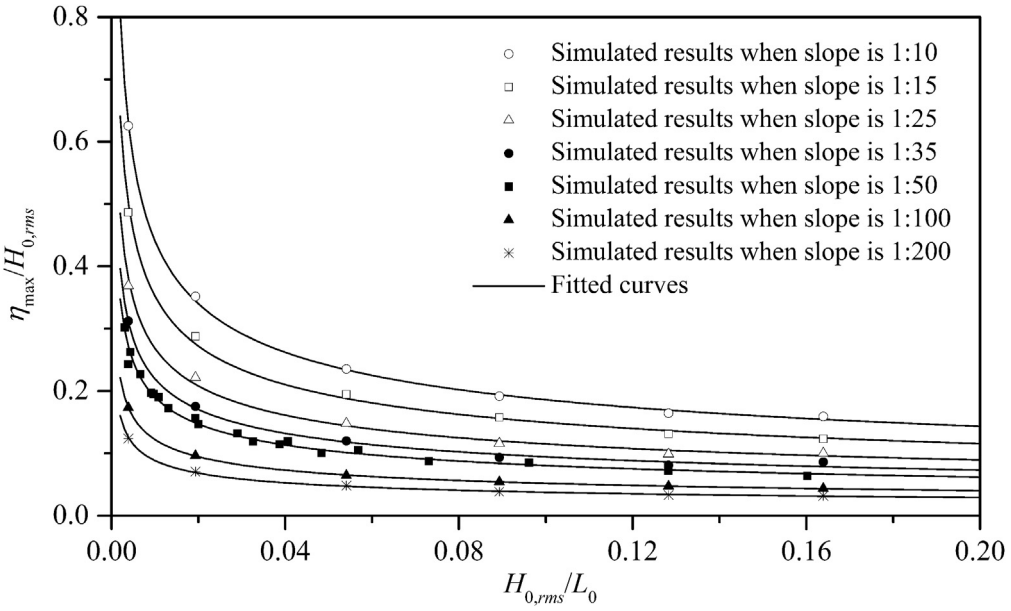

Fig. 5. Relationships between $\eta_{max}/H_{0,rms}$ and $H_{0,rms}/L_0$ for seven different beach slopes.

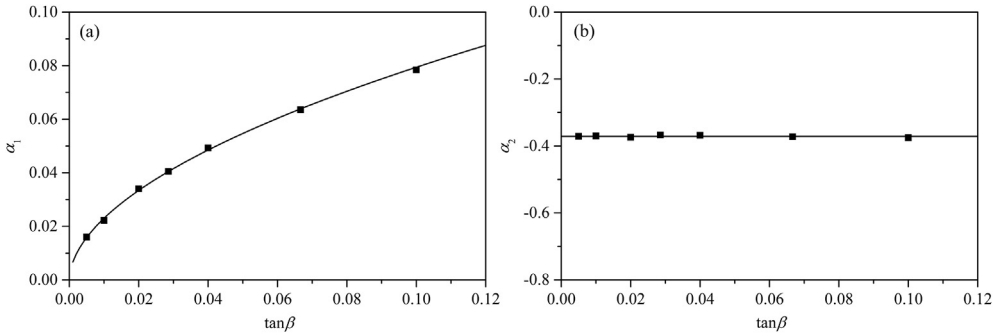

Fig. 6. Relationships between tanβ and coefficients α_1 and α_2 for seven different beach slopes.

water level with data. Following Ahmed and Sato (2003) and Bonakdar and Etemad-Shahidi (2011), this study further compares the model results with data using statistical parameters, including the index of agreement (I_a), correlation coefficient (*CC*), mean bias error (*MBE*), root mean squared error (*RMSE*) and relative root mean squared error (*RRMSE*):

$$I_a = 1 - \frac{\sum_{i=1}^{n}(x_i - y_i)^2}{\sum_{i=1}^{n}\left(|x_i - \mu_y| + |y_i - \mu_y|\right)^2} \tag{24}$$

$$CC = \frac{(1/n)\sum_{i=1}^{n}\left[(x_i - \mu_x)(y_i - \mu_y)\right]}{\sqrt{(1/n)\sum_{i=1}^{n}(x_i - \mu_x)^2}\sqrt{(1/n)\sum_{i=1}^{n}(y_i - \mu_y)^2}} \tag{25}$$

$$MBE = (1/n)\sum_{i=1}^{n}(x_i - y_i) \tag{26}$$

$$RMSE = \sqrt{(1/n)\sum_{i=1}^{n}(x_i - y_i)^2} \tag{27}$$

Table 5
Laboratory experimental conditions.

Literature	H_{rms} (m)	D (m)	T_p (sec)	tanβ
Battjes (1972)	0.073	0.55	1.51	1:20
Battjes (1974)	0.082	0.55	1.45	1:20
	0.085	0.55	2.42	1:20
Battjes and Janssen (1978)	0.144	0.705	1.84	1:20
	0.121	0.697	2.46	1:20
Stive (1985)	0.14	0.70	1.58	1:40
Shen (2015)	0.041	0.45	1.0	1:40
	0.056	0.45	1.0	1:40
	0.068	0.45	1.0	1:40
	0.045	0.45	1.5	1:40
	0.069	0.45	1.5	1:40
	0.081	0.45	1.5	1:40
	0.034	0.45	2.0	1:40
	0.057	0.45	2.0	1:40
	0.072	0.45	2.0	1:40
	0.026	0.18	1.0	1:100
	0.037	0.18	1.0	1:100
	0.026	0.18	1.5	1:100
	0.036	0.18	1.5	1:100
	0.024	0.18	2.0	1:100
	0.036	0.18	2.0	1:100

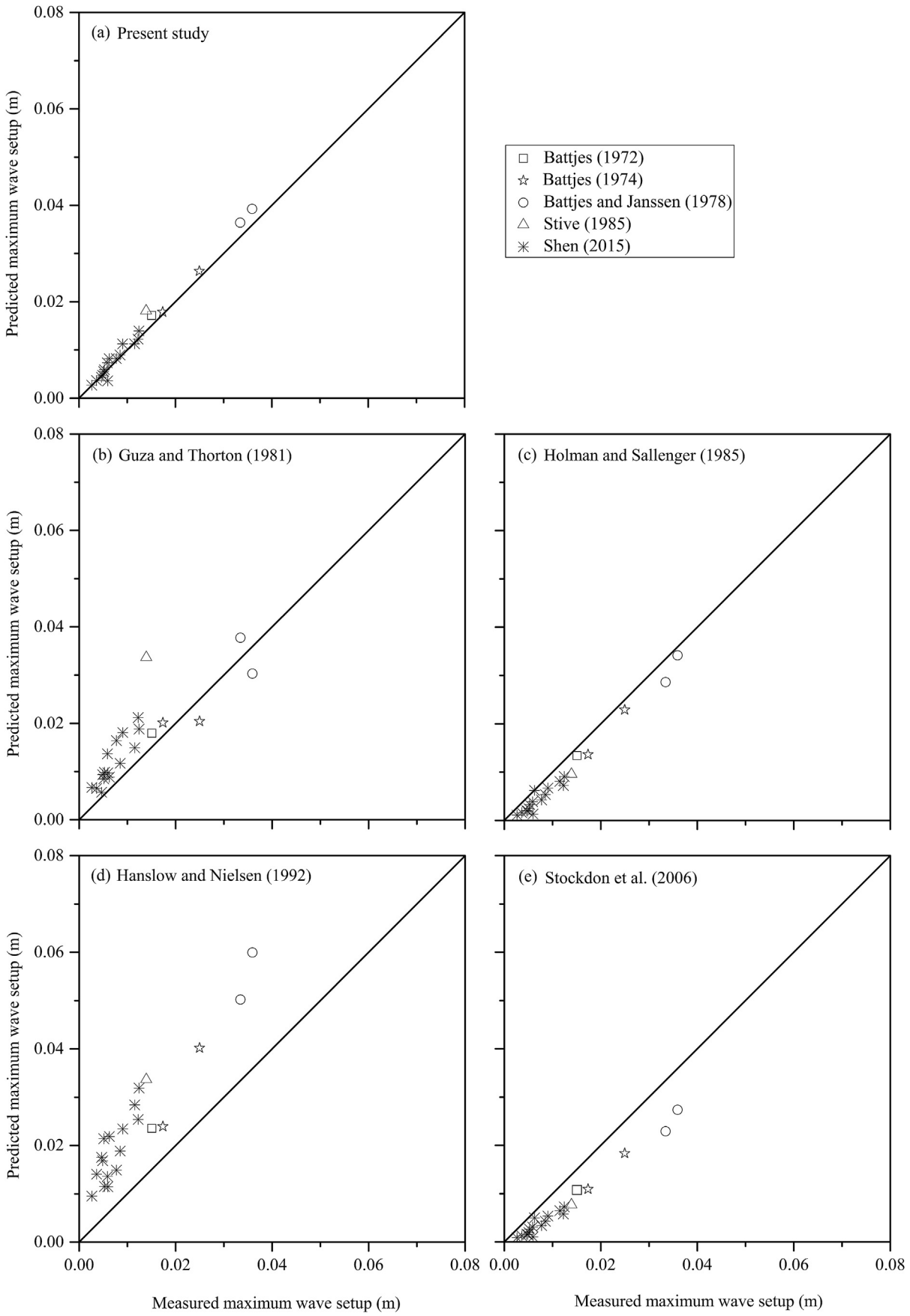

Fig. 7. Comparisons of the predicted maximum wave setup produced by different formulas and experimental measurements. The thick line is a line in agreement.

Table 6
Statistical measures between experimental measurements and empirical formulas.

Empirical formula	I_a	*CC*	*MBE* (10^{-2} m)	*RMSE* (10^{-2} m)	*RRMSE*
Present	0.99	0.99	0.17	0.10	0.12
Guza and Thornton (1981)	0.86	0.85	0.45	0.67	0.45
Holman and Sallenger (1985)	0.97	0.99	−0.28	0.31	0.21
Hanslow and Nielsen (1992)	0.73	0.94	1.27	1.36	0.92
Stockdon et al. (2006)	0.91	0.99	−0.46	0.51	0.34

$$RRMSE = \frac{\sqrt{(1/n)\sum_{i=1}^{n}(x_i - y_i)^2}}{\sqrt{(1/n)\sum_{i=1}^{n} y_i^2}} \tag{28}$$

where n is the number of the measured values; x_i and y_i denote the predicted and measured values, respectively; and μ_x and μ_y are the corresponding mean values of the predicted and measured parameters, respectively. Table 3 presents the statistical comparisons for six series of simulated results. The model results are in good agreement with observations at laboratory and field scales. The I_a and CC values are higher than 0.9 while *MBE*s, *RMSE*s and *RRMSE*s are all satisfactorily small.

3. Results

This section describes the use of the coupled model system to simulate a series of cases under controlled conditions to develop an empirical formula for the maximum wave setup. Fig. 3 shows the schematic diagram of the test beach profile. Table 4 presents the test input conditions. In the model run, the time steps for SWAN and FVCOM are 10 and 0.02 s, respectively. The time interval for information exchange between the two models is 10 s.

3.1. Result analysis

The results of Tests 25–30, shown in Fig. 4a, demonstrate the effects of the wave height on the maximum wave setup. The maximum wave setup is positively correlated with the wave height. A larger wave causes a greater wave setup. The rate of increase in the maximum setup with wave height appears to decrease with increasing wave height. Similar features can also be found for wave period and beach slope (Fig. 4b and c).

3.2. Formula development

In shore-normal wave cases, three parameters dominate the maximum wave setup: wave height, wave period and beach slope (Holman and Sallenger, 1985; Stockdon et al., 2006). An implicit function can be expressed as follows:

$$F\left(\eta_{\max}, H_{0,rms}, T_p, \tan\beta\right) = 0 \tag{29}$$

which can be transformed into a non-dimensional form:

$$F\left(\frac{\eta_{\max}}{H_{0,rms}}, \frac{H_{0,rms}}{L_0}, \tan\beta\right) = 0 \tag{30}$$

where L_0, the wavelength in deep water, is calculated as follows:

$$L_0 = \frac{gT_p^2}{2\pi} \tag{31}$$

Fig. 5 shows the relationships between $\eta_{\max}/H_{0,rms}$ and $H_{0,rms}/L_0$ in Eq. (30) for seven different beach slopes. By assuming that the relationship is simply a power-law function, the empirical formula can be expressed as

$$\frac{\eta_{\max}}{H_{0,rms}} = \alpha_1 \left(\frac{H_{0,rms}}{L_0}\right)^{\alpha_2} \tag{32}$$

in which α_1 and α_2 are undetermined coefficients related to the slope. Fig. 6 shows the fitted curves for the relationships between α_1 or α_2 and $\tan\beta$ obtained for seven different beach slopes. The parameters α_1 and $\tan\beta$ show a power function relationship, and α_2 is a constant. This study obtains the parameters using the least square method (Harris, 1998):

$$\alpha_1 = 0.274(\tan\beta)^{0.538} \tag{33}$$

$$\alpha_2 = -0.371 \tag{34}$$

Therefore, the empirical formula for the maximum wave setup becomes

$$\frac{\eta_{\max}}{H_{0,rms}} = 0.274(\tan\beta)^{0.538}\left(\frac{H_{0,rms}}{L_0}\right)^{-0.371} \tag{35}$$

After further simplification, Eq. (35) becomes the following:

$$\eta_{\max} = 0.274 H_{0,rms}^{0.629} L_0^{0.371} (\tan\beta)^{0.538} \tag{36}$$

Using $H_{0,rms} = H_{0,s}/\sqrt{2}$, Eq. (36) can be converted to a formula in terms of $H_{0,s}$:

$$\eta_{\max} = 0.220 H_{0,s}^{0.629} L_0^{0.371} (\tan\beta)^{0.538} \tag{37}$$

4. Formula evaluation

4.1. Comparison with experimental measurements

This subsection compares Eq. (36) with data collected from the different laboratory experiments listed in Table 5. Wave setup formulas developed from the literature are also compared to examine the feasibility of the formula developed in the present paper. Fig. 7 shows that Eq. (36) agrees with the laboratory data. The experimental maximum wave setup was slightly underestimated by Holman and Sallenger (1985) and Stockdon et al. (2006) but was clearly overestimated by Hanslow and Nielsen (1992). The formula of Guza and Thornton (1981) produces results comparable to the data for high wave setups but produces overestimates for low wave setups. Table 6 presents quantitative comparisons based on the five variables I_a, *CC*, *MBE*, *RMSE* and *RRMSE*. The I_a value of the present formula is as high as 0.99, which is greater than those of previous formulas, ranging from 0.73 to 0.97. The *CC* between the data and the present formula is 0.99, comparable to those presented by Holman and Sallenger (1985) and Stockdon et al. (2006) and higher than those of Guza and Thornton (1981) (0.85) and Hanslow and Nielsen (1992) (0.94). The *MBE* of the present formula is negligibly small. The *RMSE* and *RRMSE* values are 10^{-3} m and 0.12, respectively; these are much smaller than those of previously proposed formulas.

4.2. Comparison with field measurements

The present study also compares Eq. (36) with field measurements collected by Hanslow and Nielsen (1992) from sites along the New South Wales coast. Because the beach slope is non-uniform, Hanslow and Nielsen (1992) gave an approximate range of profile slopes. This paper uses the mean slope in the comparison. Fig. 8 shows the performance of different empirical formulas in determining maximum wave setup. Overall, the formula in this study shows good agreement with the data and performs better than the formula of Guza and Thornton (1981), which underestimates the wave setup compared with the observations.

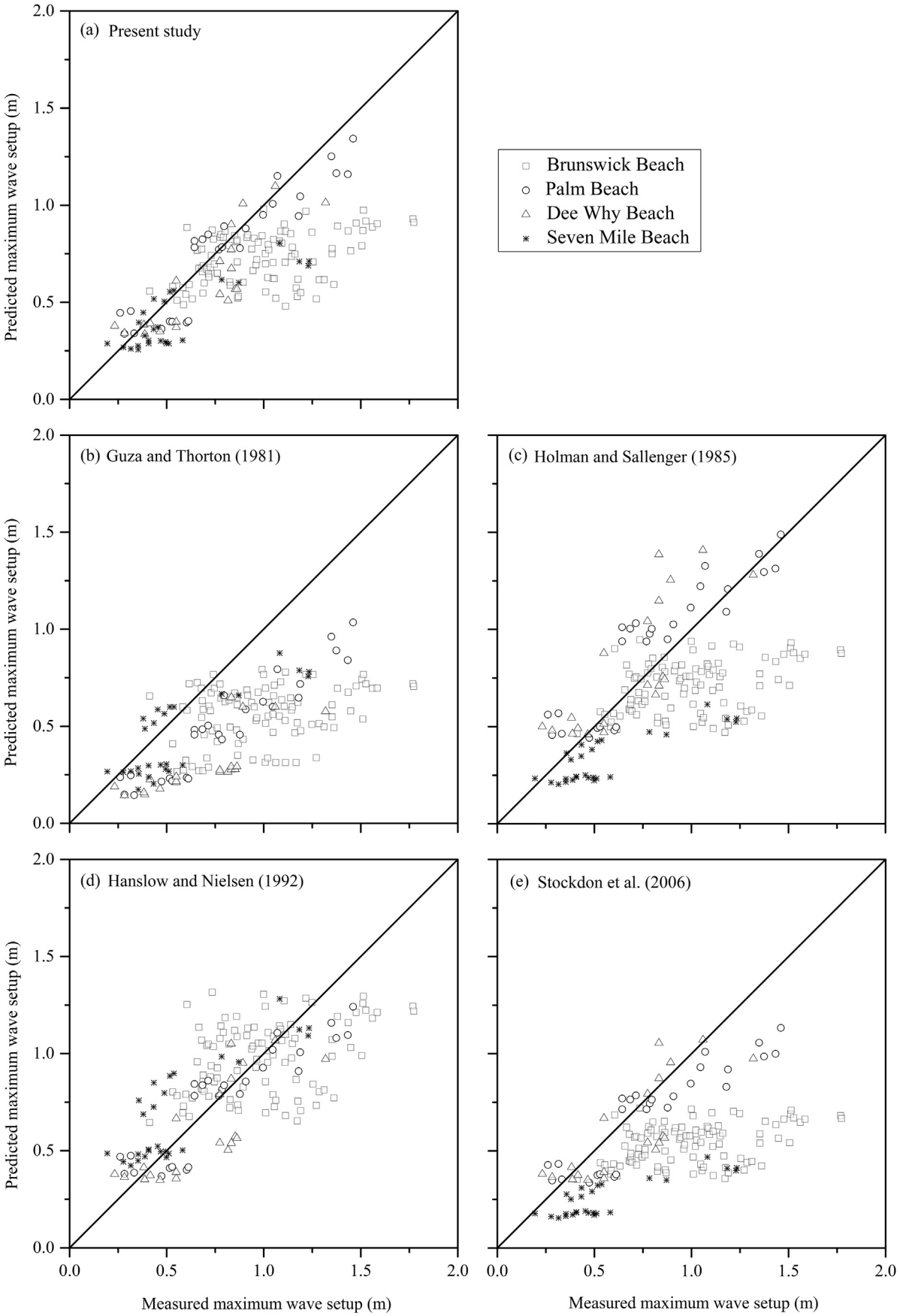

Fig. 8. Comparisons of the predicted maximum wave setup produced by different formulas and field measurements collected by Hanslow and Nielsen (1992). The thick line is a line in agreement.

Table 7
Statistical measures between field measurements and empirical formulas.

Data source	Empirical formula	I_a	*CC*	*MBE* (m)	*RMSE* (m)	*RRMSE*
Hanslow and Nielsen (1992)	Present	0.74	0.71	−0.19	0.31	0.33
	Guza and Thornton (1981)	0.60	0.64	−0.36	0.44	0.48
	Holman and Sallenger (1985)	0.70	0.56	−0.17	0.34	0.37
	Hanslow and Nielsen (1992)	0.82	0.70	−0.01	0.25	0.27
	Stockdon et al. (2006)	0.60	0.56	−0.34	0.44	0.48
Stockdon and Holman (2011)	Present	0.85	0.76	−0.02	0.19	0.33
	Guza and Thornton (1981)	0.56	0.55	−0.24	0.34	0.61
	Holman and Sallenger (1985)	0.80	0.70	0.12	0.27	0.48
	Hanslow and Nielsen (1992)	0.74	0.62	0.10	0.25	0.44
	Stockdon et al. (2006)	0.83	0.70	−0.03	0.21	0.38

The formulas of Holman and Sallenger (1985) and Stockdon et al. (2006) are satisfactory for steep slopes but underestimate the wave setup for gently sloping beaches (Brunswick Beach and Seven Mile Beach). As with the laboratory data comparison, Table 7 presents detailed comparisons based on statistical measures. The I_a value of the present formula is 0.74, which is greater than those of previous formulas except for the formula of Hanslow and Nielsen (1992) (0.82). The *CC* of the present formula (0.71) is greater than those of the other formulas. The *RMSE* and *RRMSE* values of the present formula are 0.31 m and 0.33, respectively. These two statistical values, however, are higher than those of Hanslow and Nielsen (1992). Overall, the formula of Hanslow and Nielsen (1992) seems to be slightly better than the formula of the present study. This superiority seems obvious because these authors developed their formula from the field data used here, whereas the present formula is independent of the data.

The slope data provided by Hanslow and Nielsen (1992) are approximate. This research also evaluates the proposed formula using another more accurate dataset collected by Stockdon and Holman (2011). Fig. 9 shows the comparisons of different empirical formulas and field measurements. The new formulation yields better agreement. The observations of wave setup were clearly underestimated by Guza and Thornton (1981) but were overestimated by Holman and Sallenger (1985). Table 7 presents the comparison of statistics for different formulas. The I_a and *CC* values of the present formula are 0.85 and 0.76, respectively, which are greater than those of previous formulas. The *MBE* of the present formula (−0.02 m) is negligibly small at field scale. The *RMSE* and *RRMSE* values of the present formula are 0.19 m and 0.33, respectively, which are smaller than those of the other formulas. The quantitative comparisons above show that the formula proposed in the present study is better than previous formulations, including the formula of Stockdon et al. (2006), which was developed using the same data.

5. Discussion

Based on a coupled wave-current model system, the present study proposed a new maximum wave setup formula and evaluated it against experimental and field measurements. However, the authors of this study recognize certain limitations of this approach. This section also discusses the comparisons between Eq. (36) and the formulations of Holman and Sallenger (1985) and Stockdon et al. (2006).

First, this research developed the formula based on model results under idealized conditions. By simulating a wide range of wave conditions (Table 4) and including the effects of wave breaking, bottom friction, wave-current interaction and surface rollers, certain model simplifications were present in this approach. For instance, the idealized cases used a uniform planar slope and did not consider complex bottom topography. Similarly, the development process limited the formula to the cross-shore only and used the JONSWAP spectrum to specify waves at the offshore boundary. These factors may be important for wave setup at the shoreline in certain cases (Hsu et al., 2006; Guza and Feddersen, 2012; Cox et al., 2013; Cohn and Ruggiero, 2016; Park and Cox, 2016).

Some model parameters (e.g., bottom friction in SWAN) are tunable and may have significant effects on wave propagation to influence the wave setup. Sections 2.4 and 3 have applied the default or same moderate parameters (Table 2) in all model simulations. This treatment may influence the accuracy for different cases. Overall, the purpose of this paper is to provide a general formula that can be used for practical applications and rapid computability. In the real world, simple empirical formulas may not reflect complex physical processes such as nonlinear wave and current effects. In certain cases (e.g., complex bathymetry, varied shoreline geometry, structure and strong current effects), the numerical model would provide more accurate results, although it may require a longer computation time and more detailed input information.

Second, Figs. 7–9 show that the formulations of Holman and Sallenger (1985) and Stockdon et al. (2006) also perform well considering the allowed error range. These two formulas and Eq. (36) are similar in terms of three essential factors: wave height, wavelength and beach slope are included in the formulations. Holman and Sallenger (1985) and Stockdon et al. (2006) proposed that the maximum wave setup may be directly proportional to ξ_0 (Eqs. (5) and (7)); that is, the relationship between the maximum wave setup and beach slope is linear. In the numerical model of this study, the maximum wave setup varies with the breaker index calculated by the modified Goda formula, as shown in Eqs. (11) and (12). Therefore, the maximum wave setup would have a nonlinear relationship with the slope. The empirical formula developed from the simulated results of the coupled model system certainly shows a weak nonlinear relationship between the maximum wave setup and beach slope. The maximum wave setup is approximately proportional to the square root of the slope.

The present formula indicates that the wave height is dominant compared to the wavelength. However, the formulations of Holman and Sallenger (1985) and Stockdon et al. (2006) are associated with the Iribarren parameter indicating wave height and wavelength are equally important for the maximum wave setup. This factor is an obvious difference between the formula of this study and previous formulas. Following LHS, the cross-shore gradient of the radiation stress, which is primarily influenced by the wave height, drives the wave setup. Therefore, wave height seems to be a more important factor relative to wavelength or period in determining the wave setup.

6. Conclusions

The present study developed an empirical formula for the maximum wave setup from a coupled wave-current model system based on SWAN and FVCOM. The study first evaluated the coupled model system using wave height and mean water level data collected from laboratory and field experiments covering a broad range of wave conditions. The root mean squared errors of the mean water level between the data and the counterparts from the model are less than 0.01 m, and the correlation coefficients are usually higher than 0.93. This study then used the model results based on a series of practical wave conditions to develop an empirical formula for the maximum wave setup via the least square method. The final formation of the proposed formula is $\eta_{\max} = 0.274 H_{0,rms}^{0.629} L_0^{0.371} (\tan\beta)^{0.538}$, where $H_{0,rms} = H_{0,s}/\sqrt{2}$ is the root mean square wave height for random waves in deep water, L_0 is the wavelength in deep water obtained using the peak wave period and β is the angle of the beach slope. The structure of the formula is similar to that

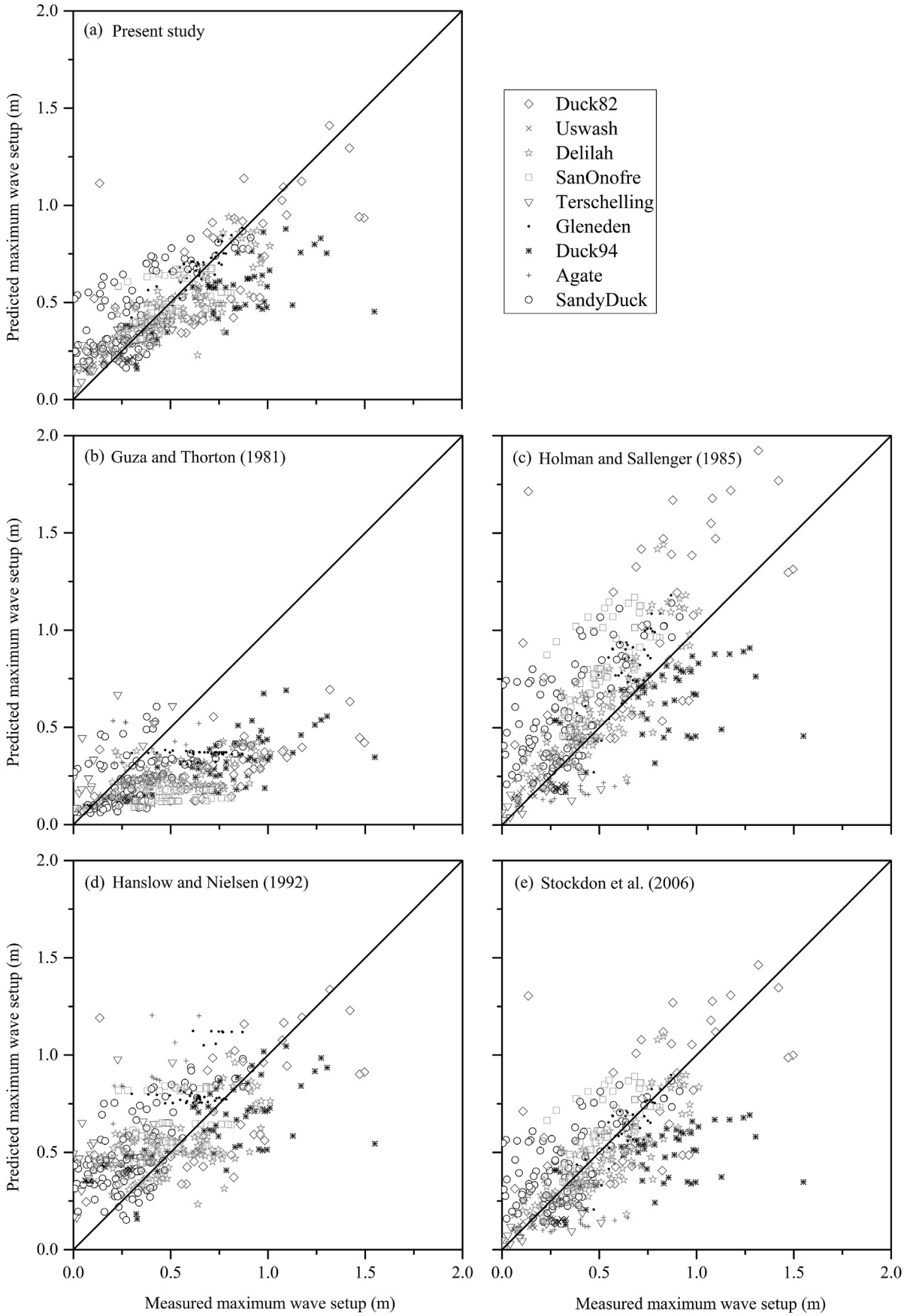

Fig. 9. Comparisons of the predicted maximum wave setup produced by different formulas and field measurements collected by Stockdon et al. (2006). The thick line is a line in agreement.

of formulas in many previous studies, but the parameter values are different. Specifically, the proposed formula shows a weak, nonlinear relationship between the maximum wave setup and the beach slope, and wave height is a more important factor than the wavelength in determining the wave setup. Using experimental and field measurements, the authors of this paper evaluated the proposed formula. The two independent field datasets cover wave heights of 0.25–4.30 m, wave periods of 3.7–17.0 s and beach slopes of 0.01–0.16. The root mean squared errors between the formula and the two sets of field observations are 0.31 and 0.19 m, and the relative root mean squared errors for both are 0.33. The proposed formula can account for most of the observed maximum wave setup. In addition, this study compared the present formula to previous formulas based on experimental and field data. The present formula is more reliable in terms of widespread applicability than previously proposed formulas.

The new empirical formula might not be applicable to complex geophysical conditions (e.g., in front of a stiff wall, structure or varied shoreline geometry). Future work will consider more practical wave, current and topographic conditions, e.g., obliquely incident waves and complex bathymetry.

Acknowledgments

The National Key Research and Development Program of China (Grant No. 2017YFC1404200), the Science Fund for Creative Research Groups of the National Natural Science Foundation of China (Grant No. 51621092) and the Open Fund of the State Key Laboratory of Hydraulic Engineering Simulation and Safety, Tianjin University (Grant No. HESS-1514) supported this research. The authors thank the anonymous reviewers for their constructive comments, especially the suggestion of using the available dataset of Stockdon and Holman (2011).

References

Ahmed, A.S.M., Sato, S., 2003. A sheet flow transport model for asymmetric oscillatory flows, Part I: uniform grains size sediments. Coast. Eng. J. 45 (3), 321–337.
Apotsos, A., Raubenheimer, B., Elgar, S., Guza, R.T., Smith, J.A., 2007. Effects of wave rollers and bottom stress on wave setup. J. Geophys. Res. 112, C02003. https://doi.org/10.1029/2006JC003549.
Battjes, J.A., 1972. Set-up due to irregular waves. In: Proc. 13th Int. Conf. On Coastal Eng. ASCE, Vancouver, pp. 1993–2004.
Battjes, J.A., 1974. Computation of Set-up, Longshore Currents, Run-up and Overtopping Due to Wind-generated Waves (Ph.D. thesis). Delft University of Technology.
Battjes, J.A., Groenendijk, H.W., 2000. Wave height distributions on shallow foreshores. Coast. Eng. 40, 61–182.
Battjes, J.A., Janssen, J.P.F.M., 1978. Energy loss and set-up due to breaking of random waves. In: Proc. 16th Int. Conf. On Coastal Eng. ASCE, Hamburg, pp. 569–587.
Bennis, A., Ardhuin, F., Dumas, F., 2011. On the coupling of wave and three-dimensional circulation models: choice of theoretical framework, practical implementation and adiabatic tests. Ocean. Modell. 40, 260–277.
Bonakdar, L., Etemad-Shahidi, A., 2011. Predicting wave run-up on rubble-mound structures using M5 model tree. Ocean. Eng. 38, 111–118.
Booij, N., Ris, R.C., Holthuijsen, L.H., 1999. A third generation wave model for coastal regions. Part 1: model description and validation. J. Geophys. Res. 104 (C4), 7649–7666.
Bowen, A.J., Inman, D.L., Simmons, V.P., 1968. Wave 'set-down' and set-up. J. Geophys. Res. 73, 2569–2577.
Calabrese, M., Vicinanza, D., Buccino, M., 2008. 2D wave setup behind submerged breakwaters. Ocean. Eng. 35 (10), 1015–1028. https://doi.org/10.1016/j.oceaneng.2008.03.005.
Chen, C., Liu, H., Beardsley, R.C., 2003. An unstructured grid, finite-volume, three-dimensional, primitive equation ocean model: application to coastal ocean and estuaries. J. Atmos. Ocean. Technol. 20, 159–186.
Chen, C., Huang, H., Beardsley, R.C., Liu, H.D., Xu, Q.C., Cowles, G., 2007. A finite volume numerical approach for coastal ocean circulation studies: comparisons with finite difference models. J. Geophys. Res. 112, C3018. https://doi.org/10.1029/2006JC003485.
Cohn, N., Ruggiero, P., 2016. The influence of seasonal to interannual nearshore profile variability on extreme water levels: modeling wave runup on dissipative beaches. Coast. Eng. 115, 79–92.
Cox, N., Dunkin, L.M., Irish, J.L., 2013. An empirical model for infragravity swash on barred beaches. Coast. Eng. 81, 44–50.
Goda, Y., 1970. A synthesis of breaker indices. Trans. Jpn. Soc. Civ. Eng. 2, 227–230.
Goda, Y., 2009. A performance test of nearshore wave height prediction with CLASH datasets. Coast. Eng. 56, 220–229. https://doi.org/10.1016/j.coastaleng.2008.07.003.
Guza, R.T., Feddersen, F., 2012. Effect of wave frequency and directional spread on shoreline runup. Geophys. Res. Lett. 39 (11).
Guza, R.T., Thornton, E.B., 1981. Wave set-up on a natural beach. J. Geophys. Res. 86 (C5), 4133–4137.
Hanslow, D.J., Nielsen, P., 1992. Wave setup on beaches and in river entrances. In: Proc. 23rd Int. Conf. On Coastal Eng. ASCE, Venice, pp. 240–252.
Harris, D.C., 1998. Nonlinear least-squares curve fitting with microsoft excel solver. J. Chem. Educ. 75 (1), 119–121.
Holman, R.A., Sallenger Jr., A.H., 1985. Setup and swash on a natural beach. J. Geophys. Res. 90 (C1), 945–953.
Hsu, T.W., Hsu, J.R.C., Weng, W.K., Wang, S.K., Ou, S.H., 2006. Wave setup and setdown generated by obliquely incident waves. Coast. Eng. 53 (10), 865–877.
Hu, K., Ding, P., Wang, Z., Yang, S., 2009. A 2D/3D hydrodynamic and sediment transport model for the Yangtze Estuary, China. J. Mar. Syst. 77, 114–136. https://doi.org/10.1016/j.jmarsys.2008.11.014.
Jacob, R., Larson, J., Ong, E., 2005. M×N communication and parallel interpolation in community climate system model version 3 using the model coupling toolkit. Int. J. High. Perform. Comput. Appl. 19, 293–307. https://doi.org/10.1177/1094342005056116.
Kumar, N., Voulgaris, G., Warner, J.C., Olabarrieta, M., 2012. Implementation of the vortex force formalism in the coupled ocean-atmosphere-wave-sediment transport (COAWST) modeling system for inner shelf and surf zone applications. Ocean. Modell. 47, 65–95.
Larson, J., Jacob, R., Ong, E., 2005. The Model Coupling Toolkit: a new Fortran90 toolkit for building multiphysics parallel coupled models. Int. J. High. Perform. Comput. Appl. 19, 277–292. https://doi.org/10.1177/1094342005056115.
Lentz, S., Raubenheimer, B., 1999. Field observations of wave setup. J. Geophys. Res. 104 (C11), 25867–25875.
Longuet-Higgins, M.S., Stewart, R.W., 1964. Radiation stresses in water waves; a physical discussion, with applications. Deep-Sea Res. 11, 529–562.
Madsen, P.A., Sørensen, O.R., Schäffer, H.A., 1997a. Surf zone dynamics simulated by a Boussinesq type model. Part I. Model description and cross-shore motion of regular waves. Coast. Eng. 32 (4), 255–287.
Madsen, P.A., Sørensen, O.R., Schäffer, H.A., 1997b. Surf zone dynamics simulated by a Boussinesq type model. Part II: surf beat and swash oscillations for wave groups and irregular waves. Coast. Eng. 32 (4), 289–319.
Mellor, G.L., 2003. The three-dimensional current and surface wave equations. J. Phys. Oceanogr. 33, 1978–1989.
Mellor, G.L., 2013. Waves, circulation and vertical dependence. Ocean. Dyn. 63 (4), 447–457. https://doi.org/10.1007/s10236-013-0601-9.
Mellor, G.L., 2015. A combined derivation of the integrated and vertically resolved, coupled wave-current equations. J. Phys. Oceanogr. 45, 1453–1463. https://doi.org/10.1175/JPO-D-14-0112.1.
Mellor, G.L., Yamada, T., 1982. Development of a turbulence closure model for geophysical fluid problems. Rev. Geophys. 20, 851–875.
Mellor, G.L., Donelan, M.A., Oey, L.Y., 2008. A surface wave model for coupling with numerical ocean circulation models. J. Atmos. Ocean. Technol. 25, 1785–1807. https://doi.org/10.1175/2008JTECHO573.1.
Moghimi, S., Klingbeil, K., Gräwe, U., Burchard, H., 2013. A direct comparison of a depth-dependent Radiation stress formulation and a Vortex force formulation within a three-dimensional coastal ocean model. Ocean. Modell. 70, 132–144.
Nielsen, P., 1988. Wave setup: a field study. J. Geophys. Res. 93 (C12), 15643–15652.
Park, H., Cox, D.T., 2016. Empirical wave run-up formula for wave, storm surge and berm width. Coast. Eng. 115, 67–78.
Raubenheimer, B., Guza, R.T., Elgar, S., 2001. Field observations of wave-driven setdown and setup. J. Geophys. Res. 106 (C3), 4629–4638.
Schäffer, H.A., Madsen, P.A., Deigaard, R., 1993. A Boussinesq model for waves breaking in shallow water. Coast. Eng. 20, 185–202.
Scott, C.P., Cox, D.T., Shin, S., Clayton, N., 2004. Estimates of surf zone turbulence in a large scale laboratory flume. In: Proc. 29th Int. Conf. On Coastal Eng. ASCE, Lisbon, pp. 379–391.
Shen, L., 2015. Study of the Feature of Longshore Current Instability on Mild Beach Slope (Ph.D. thesis). Dalian University of Technology (in Chinese).
Shen, Y., Zhang, Q., Chen, C., Ji, C., 2015. Application of modified breaking index of Goda in SWAN model. Port. Eng. Technol. (in press) (in Chinese).
Stive, M.J.F., 1985. A scale comparison of waves breaking on a beach. Coast. Eng. 9, 151–158.
Stockdon, H.F., Holman, R.A., 2011. Observations of Wave Runup, Setup, and Swash on Natural Beaches. Data Series 602U.S. Geological Survey.
Stockdon, H.F., Holman, R.A., Howd, P.A., Sallenger, A.H., 2006. Empirical parameterization of setup, swash, and runup. Coast. Eng. 53, 573–588. https://doi.org/10.1016/j.coastaleng.2005.12.005.
Svendsen, I.A., 1984. Wave heights and set-up in a surf zone. Coast. Eng. 8, 303–329.
Ting, F.C.K., 2001. Laboratory study of wave and turbulence velocity in broad-banded irregular wave surf zone. Coast. Eng. 43, 183–208.
Van Dorn, W.G., 1976. Set-up and run-up in shoaling breakers. In: Proc. 15th Int. Conf. On Coastal Eng. ASCE, Honolulu, pp. 738–751.
Warner, J.C., Sherwood, C.R., Signell, R.P., Harris, C., Arango, H.G., 2008. Development of a three-dimensional, regional, coupled wave, current, and sediment-transport model. Comput. Geosci. 34, 1284–1306. https://doi.org/10.1016/j.cageo.2008.02.012.
Wolf, J., Hubbert, K.P., Flather, R.A., 1988. A Feasibility Study for the Development of a Joint Surge and Wave Model. Proudman Oceanographic Laboratory Report, No. 1, p. 109.
Yang, J., 2012. Development and Application of a Dynamically Coupled Wave-current Model (Master's thesis). Tianjin University (in Chinese).